Is CO a Special Ligand in Organometallic Chemistry? Theoretical Investigation of AB, $Fe(CO)_4AB$, and $Fe(AB)_5$ (AB = N_2, CO, BF, SiO)

Udo Radius,[†] F. Matthias Bickelhaupt,[‡] Andreas W. Ehlers,[§] Norman Goldberg,[||] and Roald Hoffmann*

Baker Laboratory, Department of Chemistry, Cornell University, Ithaca, New York 14853-1301

Received July 18, 1997

Carbon monoxide, CO, is a ubiquitous ligand in organometallic and coordination chemistry. In the present paper we investigate the neutral isoelectronic molecules AB = N_2, CO, BF, and SiO and their coordination in the model complexes $Fe(CO)_4AB$ and $Fe(AB)_5$, using nonlocal density functional theory and a large, polarized STO basis set of triple-ζ quality (NL-SCF/TZ(2P)). Our aim is to get more insight into the ligating properties of SiO and BF in comparison to CO and N_2. The computed 298 K $Fe(CO)_4$−AB bond dissociation enthalpies of C_{3v}-symmetric $Fe(CO)_4AB$ are 18.1, 42.3, 67.9, and 35.6 kcal/mol for N_2, CO, BF, and SiO, respectively; the corresponding values for C_{2v}-symmetric $Fe(CO)_4AB$ are comparable: 19.0, 42.3, 66.7, and 39.7 kcal/mol. Good, balanced σ donation (through 5σ) and π acceptance (through 2π) are what makes CO a good donor, of course. The gap between these frontier orbitals (5σ and 2π) becomes even smaller in SiO and BF. The analysis of the bonding mechanism of the Fe−AB bond shows that SiO is a better σ donor but a worse π acceptor ligand than CO and that BF should be superior to CO in terms of both σ donor and π acceptor properties. However, these polar ligands are therefore also more reactive; and more sensitive, e.g. to nucleophilic attack, because of a low-energy 2π LUMO. Our results suggest that BF and SiO should, in principle, be excellent ligands. We also find interesting side-on and O-bound local minima, not very unstable, for SiO bound to an $Fe(CO)_4$ fragment.

1. Introduction

Carbon monoxide, CO, is ubiquitous in organometallic and coordination chemistry. It plays a key role in many catalytic processes, either as a reacting partner or as a spectator ligand. The remarkable history of the carbonyl ligand begins with Schützenberger's synthesis of $PtCl_2(CO)_2$ in 1868.[1] A further milestone in organometallic chemistry was the accidental synthesis of nickel tetracarbonyl by Mond et al. in 1890.[2] Although it was not the first transition metal carbonyl species, the remarkable properties and industrial importance of nickel tetracarbonyl, already recognized by Mond, received much attention.

Over the years, transition metal carbonyl complexes have become one of the most important families of compounds in organometallic chemistry.[3] They are common starting materials for the synthesis of other low-valent metal complexes and clusters. Carbonyl ligands may be substituted by a large number of other ligands, and in many cases these compounds are stabilized against oxidation or thermal decomposition by the remaining CO groups. Carbonyl complexes and carbonylmetalates are also useful tools for organic chemists[4]—Collman's reagent,[5] $Na_2[Fe(CO)_4]$, for example, is of importance in organic synthesis. Metal carbonyls play also an important role as intermediates in homogeneous catalytic processes.[6] A prominent example is the hydroformylation of alkenes or the "C_1 chemistry" of the so-called Fischer−Tropsch process, where CO is used as a carbon synthon to build up alkanes, olefins, and alcohols.[7]

Nowadays, ligands isoelectronic to CO are also quite well-known in metal compounds (cf. Werner for an excellent

[†] Present address: Institut für Anorganische Chemie, Universität Karlsruhe (T.H.), Engesserstrasse, Geb. 30.45, D-76128 Karlsruhe, Germany.

[‡] Present address: Fachbereich Chemie, Philipps-Universität Marburg, Hans-Meerwein-Strasse, D-35032 Marburg, Germany.

[§] Present address: Afdeling Theoretische Chemie, Scheikundig Laboratorium der Vrije Universiteit, De Boelelaan 1083, NL-1081 HV Amsterdam, The Netherlands.

[||] Present address: Institut für Organische Chemie, Technische Universität Braunschweig, Hagenring 30, D-38106 Braunschweig, Germany.

(1) Schützenberger, M. P. *Annales (Paris)* **1868**, *15*, 100.

(2) Mond, L.; Langer, C.; Quinke, F. *J. Chem. Soc.* **1890**, 749.

(3) (a) Greenwood, N. N.; Earnshaw, A. *Chemistry of the Elements*; Pergamon: Oxford, U.K., 1989. (b) Huheey, J. E. *Inorganic Chemistry: Principles of Structure and Reactivity*, 3rd ed.; Harper & Row: New York, 1983; Chapter 13. (c) Cotton, F. A.; Wilkinson, G. *Advanced Inorganic Chemistry*, 5th ed.; Wiley: New York, 1988. (d) Purcell, K. F.; Kotz, J. C. *Inorganic Chemistry*; W. B. Saunders: Philadelphia, PA, 1977. (e) Crabtree, R. H. *The Organometallic Chemistry of the Transition Metals*, 2nd ed.; Wiley: New York, 1994; especially Chapters 4, 7.1, 8.1, 12, and 13. (f) Elschenbroich, Ch.; Salzer, A.; *Organometallics. A Concise Introduction*, 2nd ed.; Verlag Chemie: Weinheim, Germany, 1992; Chapter 14.5, 16. (g) Collman, J. P.; Hegedus, L. S.; Norton, J. R.; Finke, R. G. *Principles and Applications of Organotransition Metal Chemistry*; University Science Books: Mill Valley, CA, 1987. (h) Haiduc, I.; Zuckerman, J. J. *Basic Organometallic Chemistry*; de Gruyter: Berlin, 1985; Chapter 11.1. (i) Hartley, F. R., Patai, S., Eds. *The Chemistry of the Metal Carbon Bond, Vol. 1: The Structure, Preparation, Thermochemistry, and Characterization of Organometallic Compounds*; Wiley: New York, 1982. (j) Hartley, F. R., Patai, S., Eds. *The Chemistry of the Metal Carbon Bond, Vol. 2: The Nature and Cleavage of Metal−Carbon Bonds*; Wiley: New York, 1985; Especially for iron carbonyls see for example: (k) Abel, E. W.; Stone, F. G. A.; Wilkinson, G.; *Comprehensive Organometallic Chemistry*; Pergamon: New York, 1982; Vol. 4, Chapter 31. (l) Abel, E. W.; Stone, F. G. A.; Wilkinson, G. *Comprehensive Organometallic Chemistry II*; Elsevier: New York, 1995; Vol. 7, Chapter 1−4. For a historical perspective see for example: (m) Thayer, J. S. *Adv. Organomet. Chem* **1975**, *13*, 1. (n) Parshall, G. W. *Organometallics* **1987**, *6*, 697. (o) For a discussion of electrostatic effects on the C−O bond strength in cationic complexes, see: Goldman, A. S.; Krogh-Jespersen, K. *J. Am. Chem. Soc.* **1996**, *118*, 12159.

S0020-1669(97)00897-5 CCC: $15.00
Published on Web 02/13/1998

review[8a]), among them relatively stable molecules such as N_2, NO^+, and CN^-, as well as less stable species such as vinylidene CCH_2.[8] However, the number of complexes with *neutral* isoelectronic diatomic molecules terminally ligated to transition metals is somewhat limited, mainly restricted to complexes with ligands of the type CE (E = S, Se, Te, NR, CH_2) and N_2. None of these other ligands seems to be as versatile as CO.

What, besides its excellent experimental accessibility, makes CO such a special ligand in organometallic chemistry? In what way are other diatomic ligands, such as N_2, BF, and SiO, similar to or different from CO? Is it possible to trace the versatility of carbon monoxide to distinct features in its electronic structure, and can (some of) these features be found in other ligands, too? To answer these and other questions, we have carried out a careful theoretical investigation, using density functional theory (DFT) on C_{3v}- (**1**) and C_{2v}-symmetric $Fe(CO)_4AB$ (**2**), as well as the homoleptic $Fe(AB)_5$ (**3**) series (Chart 1) for AB = N_2, CO, BF, and SiO. We aspire to a chemically meaningful analysis of the bonding in these molecules.

Some of our model systems are of course known molecules. The simplest, $Fe(CO)_5$ (**3b**), was independently detected by Mond and by Berthelot in 1891.[9] Both $Fe(CO)_4(N_2)$ (**1a**)[10] and the thermally unstable $Fe(N_2)_5$ (**3a**)[11] have been observed in matrices. The latter is presumed to be isostructural to $Fe(CO)_5$ with terminal N_2 ligands. For $Fe(CO)_4(N_2)$ a C_{3v} structure with an axial N_2 ligand was suggested on basis of IR data.[10]

Chart 1

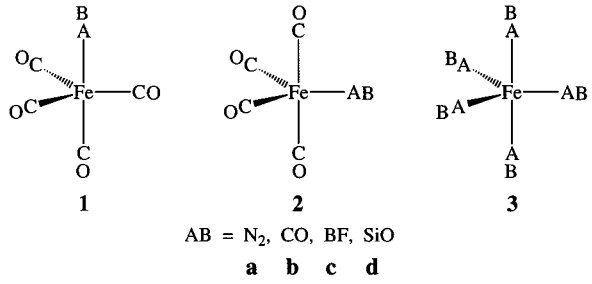

The other model systems are hitherto unknown, although transition metal complexes with SiO ligands have been observed recently in an argon matrix by the Schnöckel group.[12] Also, Schmid, Petz, and Nöth have reported a thermolabile compound of the composition $Fe(CO)_4(BNR_2)$ (R = Me, Et) in 1970[13] containing the BNR_2 ligand, which is isoelectronic to BF.

Why have we chosen the iron system for our initial studies? First, as mentioned above, the BNR_2 ligands are actually known for iron. Second, we wanted to choose a system in which we could right away address the stereochemical richness resulting from differentiated axial and equatorial substitution. We have not neglected the well-known and symmetrical $Cr(CO)_5AB$ and $Ni(CO)_3AB$ alternatives; these in fact are studied in a subsequent paper in the series.[14]

2. Theoretical Methods

A. General Procedure. All calculations were performed using the Amsterdam-Density-Functional (ADF) program[15] developed by Baerends et al.,[15a−d] vectorized by Ravenek,[15e] and parallelized by Fonseca Guerra et al.[15a] The numerical integration was performed using the procedure developed by te Velde et al.[15f,g] The MOs were expanded in a large uncontracted set of Slater type orbitals (STOs) containing diffuse functions: TZ(2P).[15h] The basis set is of triple-ζ quality for all atoms and has been augmented with two sets of polarization functions (i.e. 3d and 4f) on B, C, N, O, F, and Si. The 1s core shell of boron, carbon, nitrogen, oxygen, and fluorine and the 1s2s2p core shells of silicon and iron were treated by the frozen-core approximation.[15b] An auxiliary set of s, p, d, f, and g STOs was used to fit the molecular density and to represent the Coulomb and exchange potentials accurately in each SCF cycle.[15i]

Geometries and energies were calculated using nonlocal density functionals (NL). Equilibrium structures were optimized using analytical gradient techniques.[15j] Frequencies[15k] were calculated by numerical differentiation of the analytical energy gradients and using the local density approximation (LDA).[15l,m]

At the LDA level exchange is described by Slater's Xα potential[16] and correlation is treated in the Vosko−Wilk−Nusair (VWN) parametrization.[15n] At the NL-SCF level nonlocal corrections for the

(4) (a) Crabtree, R. H. *The Organometallic Chemistry of the Transition Metals*, 2nd ed.; Wiley: New York, 1994; Chapter 14. (b) Wender, I.; Pino, P. *Organic Syntheses via Metal Carbonyls*; Wiley: New York, 1968, 1977; Vols. I and II. (c) Alper, H. *Transition Metal Organometallics in Organic Synthesis*; Academic Press: New York, 1976, 1978. (d) Davies, S. G. *Organotransition Metal Chemistry: Applications to Organic Synthesis*; Pergamon: Oxford, U.K., 1982. (e) Hartley, F. R., Patai, S., Eds. *The Chemistry of the Metal Carbon Bond, Vol. 4: The Use of Organometallic Compounds in Organic Synthesis*; Wiley: New York, 1987. (f) Hartley, F. R., Patai, S., Eds. *The Chemistry of the Metal Carbon Bond, Vol 5: Organometallic Compounds in Organic and Biological Synthesis*; Wiley: New York, 1989. (g) de Meijere, A., tom Dieck, H., Eds. *Organic Synthesis via Organometallics*; Springer: Berlin, 1987. (h) Werner, H., Erker, G., Eds. *Organic Synthesis via Organometallics*; Springer: Berlin, 1989. (i) Dötz, K. H., Hoffmann, R. W., Eds. *Organic Synthesis via Organometallics*; Springer: Berlin, 1991.
(5) Collman, J. P. *Acc. Chem. Res* **1975**, *8*, 342.
(6) (a) Elschenbroich, Ch.; Salzer, A. *Organometallics. A Concise Introduction*, 2nd ed.; Verlag Chemie: Weinheim, Germany, 1992; Chapter 17. (b) Crabtree, R. H. *The Organometallic Chemistry of the Transition Metals*, 2nd ed.; Wiley: New York, 1994; especially Chapter 9. (c) Parshall, G. W.; Ittel, S. T. *Homogeneous Catalysis. The Applications and Chemistry by Soluble Transition Metal Complexes*; Wiley: New York, 1992; especially Chapter 5. (d) Moser, W. R., Slocum, D. W., Eds. *Homogeneous Transition Metal Catalyzed Reactions*; American Chemical Society: Washington, DC, 1992. (e) Hartley, F. R., Patai, S., Eds. *The Chemistry of the Metal Carbon Bond, Vol. 3: Carbon−Carbon Bond Formation using Organometallic Compounds*; Wiley: New York, 1985.
(7) (a) Fischer, F.; Tropsch, H. *Brennst. Chem.* **1923**, *4*, 276. (b) Fischer, F.; Tropsch, H. *Brennst. Chem.* **1926**, *7*, 97. (c) Fischer, F.; Tropsch, H. *Chem. Ber.* **1926**, *59*, 836. (d) Elschenbroich, Ch.; Salzer, A. *Organometallics. A Concise Introduction*, 2nd ed.; Verlag Chemie: Weinheim, Germany, 1992; Chapter 17.9, 17.12. (e) Keim, W., Ed. *Catalysis in C_1 Chemistry*; Reidel: Dordrecht, The Netherlands, 1983. (f) Sheldon, R. A. *Chemicals from Synthesis Gas: Catalytic Reactions of CO and H_2*; Reidel: Dordrecht, The Netherlands, 1983. (g) Anderson, R. B. *The Fischer−Tropsch Synthesis*; Academic Press: Orlando, FL, 1984. (h) Guczi, L., Ed. *New Trends in CO Activation*; Elsevier: New York, 1991. (i) Braca, G., Ed. *Oxygenates by Homologation or CO Hydrogenation with Metal Complexes*; Kluwer: Dordrecht, The Netherlands, 1994. (j) Ford, P. C. *Acc. Chem. Res.* **1981**, *14*, 31. (k) Hermann, W. A. *Angew. Chem.* **1982**, *94*, 118; *Angew. Chem., Int. Ed. Engl.* **1982**, *21*, 117. (l) Goodman, D. W. *Acc. Chem. Res.* **1984**, *17*, 194. (m) Ford, P. C.; Rokicki, A. *Adv. Organomet. Chem.* **1988**, *28*, 139. (n) Cornils, B.; Hermann, W. A.; Rasch, M. *Angew. Chem.* **1994**, *106*, 2219; *Angew. Chem., Int Ed. Engl.* **1994**, *33*, 2144.
(8) (a) Werner, H. *Angew. Chem.* **1990**, *102*, 1109; *Angew. Chem., Int. Ed. Engl.* **1990**, *29*, 1077. (b) Ehlers, A. W.; Dapprich, S.; Vyboishchikov, S. F.; Frenking, G. *Organometallics* **1996**, *15*, 105.
(9) (a) Mond, L.; Quincke F. *J. Chem. Soc.* **1891**, *59*, 604. (b) Berthelot, M. *C. R. Hebd. Seances Acad. Sci.* **1891**, *112*, 343.
(10) Poliakoff, M.; Turner, J. J. *J. Chem. Soc., Dalton Trans.* **1974**, 2276−2285.
(11) Doeff, M. M.; Parker, S. F.; Barett, P. H.; Pearson, R. G. *Inorg. Chem.* **23**, *1984*, 4108.
(12) (a) Mehner, T.; Köppe, R.; Schnöckel, H. *Angew. Chem.* **1992**, *104*, 653; *Angew. Chem., Int. Ed. Engl.* **1992**, *31*, 638. (b) Mehner, T.; Schnöckel, H.; Almond, M. J. *J. Chem. Soc., Chem. Commun.* **1988**, 117.
(13) Schmid, G.; Petz, W.; Nöth, H. *Inorg. Chim. Acta* **1970**, *4*, 423.
(14) (a) Bickelhaupt, F. M.; Radius, U.; Ehlers, A. W.; Hoffmann, R.; Baerends, E. J. *New. J. Chem.*, in press. (b) Ehlers, A. W.; Baerends, E. J.; Bickelhaupt, F. M.; Radius, U. *Chem.—Eur. J.*, in press.

exchange due to Becke[15o,p] and for correlation due to Perdew[15q] are added self-consistently.[15r]

Atomic ground-state energies were corrected for the fact that present day approximate density functionals are in general not invariant over the set of densities belonging to a degenerate ground state. As a consequence, there may be uncertainties in the order of 3−5 kcal/mol in atomic ground-state energies.[15s,t] Our atomic ground-state energies were accordingly adjusted using the corrections recommended by Baerends et al.[15s] (in kcal/mol): −4.6 (B ^{2}P), −6.2 (F ^{2}P), −3.5 (C ^{3}P), −8.5 (O ^{3}P), −1.4 (Si ^{3}P), 0.0 (N ^{4}S), and −10.8 (Fe ^{5}D(s^2d^6)) with respect to the spherical spin polarized atom.

Bond enthalpies at 298.15 K and 1 atm (ΔH_{298}) were calculated from 0 K electronic bond energies (BE) according to eq 1, assuming an ideal gas.[17]

$$\Delta H_{298} = \mathrm{BE} + \Delta E_{\mathrm{trans},298} + \Delta E_{\mathrm{rot},298} + \Delta E_{\mathrm{vib},0} + \Delta(\Delta E_{\mathrm{vib}})_{298} + \Delta(pV) \quad (1)$$

Here, $\Delta E_{\mathrm{trans},298}$, $\Delta E_{\mathrm{rot},298}$, and $\Delta E_{\mathrm{vib},0}$ are the differences between products and reactants in translational, rotational, and zero point vibrational energy, respectively; $\Delta(\Delta E_{\mathrm{vib}})_{298}$ is the change in the vibrational energy difference as one goes from 0 to 298.15 K. The vibrational energy corrections are based on our frequency calculations. The molar work term $\Delta(pV)$ is $(\Delta n)RT$; $\Delta n = -1$ for two fragments combining to one molecule. Thermal corrections for the electronic energy are neglected as well as contributions due to the basis set superposition error (BSSE). A recent investigation on the first bonding energy of $Cr(CO)_5$−CO of Baerends et al.[15u] shows that the BSSE is of the magnitude of 1 kcal/mol for the basis set combination used in this study.

B. Bonding Energy Analysis. The bonding in the various $Fe(CO)_4AB$ and $Fe(AB)_5$ systems was analyzed using an extended transition state (ETS) method developed by Ziegler and Rauk.[18] The overall bond energy ΔE is made up of two major components (eq 2).

$$\Delta E = \Delta E_{\mathrm{prep}} + \Delta E_{\mathrm{int}} \quad (2)$$

In this formula the preparation energy ΔE_{prep} is the amount of energy required to deform the separated fragments from their equilibrium structure to the geometry that they acquire in the overall molecule. The interaction energy ΔE_{int} corresponds to the actual energy change when the prepared fragments are combined to form the overall molecule. The interaction energy is further split up into two physically meaningful terms (eq 3):

$$\Delta E_{\mathrm{int}} = \Delta E_{\mathrm{elst}} + \Delta E_{\mathrm{Pauli}} + \Delta E_{\mathrm{oi}} = \Delta E^\circ + \Delta E_{\mathrm{oi}} \quad (3)$$

The term ΔE_{elst} corresponds to the classical electrostatic interaction between the unperturbed charge distributions of the prepared fragments and is usually attractive. The Pauli-repulsion $\Delta E_{\mathrm{Pauli}}$ comprises the four-electron destabilizing interactions between occupied orbitals and is responsible for the steric repulsion. For neutral fragments, it is useful to combine ΔE_{elst} and $\Delta E_{\mathrm{Pauli}}$ in a "steric interaction" term ΔE° (eq 3). The orbital interaction ΔE_{oi} accounts for charge transfer (interaction between occupied orbitals on one moiety with unoccupied orbitals of the other, including the HOMO−LUMO interactions) and polarization (empty/occupied orbital mixing on one fragment). It can be decomposed into the contributions from each irreducible representation Γ of the interacting system (eq 4).[18a−d] In systems with a clear σ, π separation this symmetry partitioning proves to be most informative.

$$\Delta E_{\mathrm{oi}} = \sum \Delta E_\Gamma \quad (4)$$

The NL-SCF/TZ(2P) electron density was also analyzed using the Hirshfeld method for the computation of atomic charges.[18e]

3. Bonding in the Isolated Diatomics

A. N_2, CO, and BF. Our purpose is to compare isoelectronic compounds containing direct main group−transition metal bonding, to point out similarities in the way related fragments combine and to determine in what ways the members of the isoelectronic series $Fe(CO)_4AB$ and $Fe(AB)_5$ (AB = CO, SiO, NN, and BF) differ. It is instructive to preface our detailed analysis of the complexes with some considerations emerging from the free ligands. This account is certainly familiar for CO and N_2 and probably somewhat less so for SiO and BF.[19] Then we will describe calculated geometries, bonding energies, and selected frequencies of the complexes $Fe(CO)_4AB$ and $Fe(AB)_5$.

Our computational results for the diatomics are not presented in detail here but are given in Table 5 of the Supporting Information. In general we get good to excellent agreement with experimental geometries, bonding energies, vibrational frequencies, and dipole moments of these molecules.

(15) (a) Fonseca Guerra, C.; Visser, O.; Snijders, J. G.; te Velde, G.; Baerends, E. J. Parallelisation of the Amsterdam Density Functional Program. In *Methods and Techniques for Computational Chemistry*; Clementi, E., Corongiu, G., Eds.; STEF: Cagliari, Italy, 1995; pp 305−395. (b) Baerends, E. J.; Ellis, D. E.; Ros, P. *Chem. Phys.* **1973**, *2*, 41. (c) Baerends, E. J.; Ros, P. *Chem. Phys.* **1975**, *8*, 412. (d) Baerends, E. J.; Ros, P. *Int. J. Quantum Chem., Quantum Chem. Symp.* **1978**, *S12*, 169. (e) Ravenek, W. In *Algorithms and Applications on Vector and Parallel Computers*; Riele, H. H. J., Dekker, Th. J., van de Vorst, H. A., Eds.; Elsevier: Amsterdam, 1987. (f) Boerrigter, P. M.; te Velde, G.; Baerends, E. J. *Int. J. Quantum Chem.* **1988**, *33*, 87. (g) te Velde, G.; Baerends, E. J. *J. Comput. Phys.* **1992**, *99*, 84. (h) Snijders, J. G.; Baerends, E. J.; Vernooijs, P. *At. Nucl. Data Tables* **1982**, *26*, 483. (i) Krijn, J.; Baerends, E. J. *Fit-Functions in the HFS-Method*; Internal Report (in Dutch); Vrije Universiteit: Amsterdam, 1984. (j) Versluis, L.; Ziegler, T. *J. Chem. Phys.* **1988**, *88*, 322. (k) Fan, L.; Versluis, L.; Ziegler, T.; Baerends, E. J.; Ravenek, W. *Int. J. Quantum Chem., Quantum Chem. Symp.* **1988**, *S22*, 173. (l) Bérces, A.; Ziegler, T.; Fan, L. *J. Phys. Chem.* **1994**, *98*, 1584. (m) Bérces, A.; Ziegler, T. *J. Phys. Chem.* **1994**, *98*, 13233. (n) Vosko, S. H.; Wilk, L.; Nusair, M. *Can. J. Phys.* **1980**, *58*, 1200. (o) Becke, A. D. *J. Chem. Phys.* **1986**, *84*, 4524. (p) Becke, A. D. *Phys. Rev. A* **1988**, *38*, 3098. (q) Perdew, J. P. *Phys. Rev. B* **1986**, *33*, 8822. Erratum: *Ibid.* **1986**, *34*, 7406. (r) Fan, L.; Ziegler, T. *J. Chem. Phys.* **1991**, *94*, 6057. (s) Baerends, E. J.; Branchadell, V.; Sodupe, M.; *Chem. Phys. Lett.* **1997**, *265*, 481. (t) Ziegler, T.; Rauk, A.; Baerends, E. J. *Theor. Chim. Acta* **1977**, 43, 261. (u) Rosa, A.; Ehlers, A. W.; Baerends, E. J.; Snijders, J. G.; te Velde, G. *J. Chem. Phys.* **1996**, *100*, 5690.

(16) Slater, J. C. *Quantum Theory of Molecules and Solids*; McGraw-Hill: New York, 1974; Vol. 4.

(17) Atkins, P. W. *Physical Chemistry*; Oxford University Press: Oxford, U.K., 1982.

(18) (a) Bickelhaupt, F. M.; Nibbering, N. M. M.; van Wezenbeek, E. M.; Baerends, E. J. *J. Phys. Chem.* **1992**, *96*, 4864. (b) Ziegler, T.; Rauk, A. *Inorg. Chem.* **1979**, *18*, 1558. (c) Ziegler, T.; Rauk, A. *Inorg. Chem.* **1979**, *18*, 1755. (d) Ziegler, T.; Rauk, A. *Theor. Chim. Acta* **1977**, *46*, 1. (e) Hirshfeld, F. L. *Theor. Chim. Acta* **1977**, 44, 129.

(19) (a) Albright, T. A.; Burdett, J. K.; Whangbo, M.-H. *Orbital Interactions in Chemistry*; Wiley: New York, 1985; Chapter 6. (b) Mulliken, R. S.; Ermler, W. C. *Diatomic Molecules−Results of ab Initio Calculations*; Academic Press: New York, 1977. See also for example: (c) Heinzmann, R.; Ahlrichs, R. *Theor. Chim. Acta* **1976**, *42*, 33. (d) Rozendaal, A.; Ros, P. *Acta Crystallogr.* **1982**, *A38*, 372. (e) Rozendaal, A.; Baerends, E. J. *Chem. Phys.* **1984**, *87*, 263. (f) Rozendaal, A.; Baerends, E. J. *Chem. Phys.* **1985**, *95*, 57. (g) Baerends, E. J.; Vernooijs, P.; Rozendaal, A.; Boerrigter, P. M.; Krijn, M.; Feil, D.; Sundholm, D. *J. Mol. Struct. (THEOCHEM)* **1985**, *133*, 147. (h) Rozendaal, A. Thesis; A momentum-space view of the chemical bond. II. The 14-electron diatomics BF, CO and N_2. Vrije Universiteit, Amsterdam, 1985; Chapter 6. (i) Botschwina, P. *J. Mol. Spectrosc.* **1986**, *118*, 76. (j) Ahlrichs, R.; Jankowski, K.; Wasilewski, J. *Chem. Phys.* **1987**, *111*, 263. (k) Langhoff, S. R.; Bauschlicher, C. W., Jr.; Taylor, P. R. *Chem. Phys. Lett.* **1987**, *135*, 543. (l) Cooper, D. L.; Kirby, K. *J. Chem. Phys.* **1987**, *87*, 424. (m) Wong, M. W.; Nobes, R. H.; Bouma, W. J.; Radom, L. *J. Chem. Phys.* **1989**, *91*, 2971. (n) Schnöckel, H.; Köppe, R. *J. Am. Chem. Soc.* **1989**, *111*, 4583. (o) Wang, J.; Eriksson, L. A.; Johnson, B. G.; Boyd, R. J. *J. Phys. Chem.* **1996**, *100*, 5274. (p) Li, Z.; Tao, F.-M.; Pan, Y.-K. *Int. J. Quantum Chem.* **1996**, *57*, 207. (q) Wang, J.; Clark, B. J.; Schmider, H.; Smith, V. H., Jr. *Can. J. Chem.* **1996**, *74*, 1187. (r) Filippi, C.; Umrigar, C. J. *J. Chem. Phys.* **1996**, 105, 213.

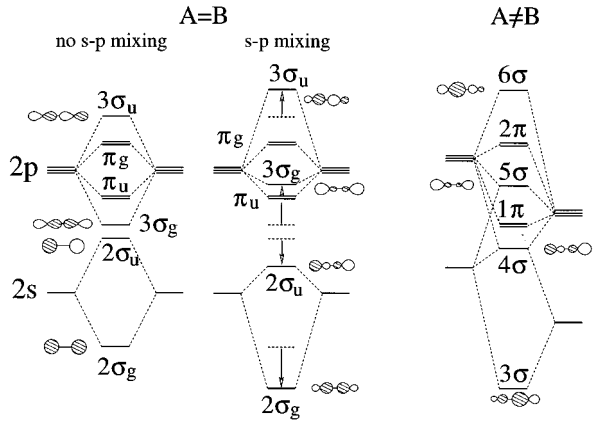

Figure 1. Schematic FMO diagrams of diatomic molecules AB built up from the atomic components A and B. Shown are the FMO diagrams of homodinuclear molecules (A = B), without s−p mixing (left side) with s−p mixing (middle), as well as the schematic FMO diagram of a heterodinuclear molecule AB (right side).

The energy levels of the ligand are important in their interactions with an $M(L)_n$ fragment, so we examine these in some detail. Figure 1 shows how the A−B orbital interactions form four σ and two π valence MOs.

Let us begin with the nitrogen molecule as a homonuclear diatomic A−B (A = B). The familiar zeroth order picture of a diatomic (left side of Figure 1) must be augmented with first-order mixing of orbitals of the same symmetry, which leads to s−p hybridization. There is substantial mixing of $2\sigma_g$ with $3\sigma_g$ and of $2\sigma_u$ with $3\sigma_u$. In each case the lower orbital is stabilized, increasing the bonding (or decreasing the antibonding) within that orbital. Thus $2\sigma_g$ becomes a better N−N σ-bond and $2\sigma_u$ a lone pair combination instead of an antibonding orbital; $3\sigma_g$ can also be viewed as a lone pair combination and is pushed above π_u, and $3\sigma_u$ forms the strongly N−N antibonding orbital. For N_2, with 10 electrons in its valence shell, $3\sigma_g$ is the HOMO of the diatomic.

The right side of Figure 1 shows an FMO diagram for heterodinuclear diatomics AB. Now there is a reduction of symmetry from $D_{\infty h}$ to $C_{\infty v}$, so the orbital labels change from $2\sigma_g$, $2\sigma_u$, π_u, $3\sigma_g$, π_g, and $3\sigma_u$ to 3σ, 4σ, 1π, 5σ, 2π, and 6σ, respectively. For simplicity, we will refer in the subsequent discussion also to the orbitals of N_2 according to this symmetry-reduced labeling scheme. Not only in N_2, but also in the other diatomics studied here, MO 5σ lies higher in energy than 1π and, in fact, represents the HOMO for the "10 electron" diatomics under investigation. Its character changes, however, as we go from N_2 to the heterodiatomics.

The lower symmetry (as well as the electronegativity differences between A and B) leads to a slightly more complicated pattern of A−B orbital interactions. Along the series N_2, CO, SiO, and BF, the A−B electronegativity difference increases monotonically from 0.0 to 2.1 (we use Allen's spectroscopic electronegativities[22]). Thus, along this series, the atomic orbitals (AOs) of the more electropositive A are higher in energy, whereas the AOs of the more electronegative B are lower in energy.

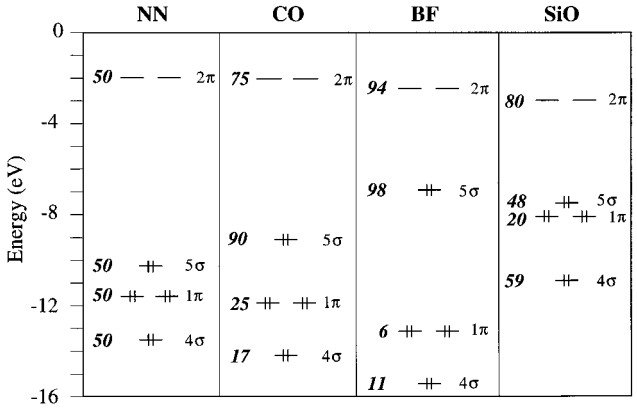

Figure 2. Calculated NL-SCF/TZ2P MO energies of AB (=N_2, CO, BF, SiO) in the range between −16 and 0 eV. The extent (percentage over all AOs) to which each MO is centered on the more electropositive atom A is given in italics.

The effect of this variation in electronegativity can be viewed as a perturbation on our zeroth order interaction picture. AO 2s of the more electropositive atom A rises and comes close in energy to the stabilized $2p_z$ of the more electronegative atom B. Now, as A and B interact, the bonding $2p_z(A) - 2p_z(B)$ combination (the coordinate system has z along the bond axis, in the same direction for A and B atoms; the main character of the MO is given, before s,p mixing) may drop below the antibonding 2s(A) − 2s(B). In other words, in the heterodiatomics the 5σ HOMO may to zeroth order be given by the antibonding 2s(A) − 2s(B) combination and not, as in N_2, by the bonding $2p_z(A) - 2p_z(B)$, which instead becomes the 4σ.

The consequences of this electronegativity perturbation are changes in the energies of molecular orbitals and in the localization of the MOs. Figure 2 shows the calculated MO energies in the range between −16 and 0 eV; we also show in this figure the extent (percentage, summed over all AOs on an atom) to which each MO is centered on the more electropositive atom A.

A general and useful rule of orbital interaction is that if one has an "electronegativity perturbation", the more bonding of a pair of molecular orbitals (σ or π bonds, lone pairs) becomes more localized on the more electronegative atom,[23] and the upper member of the pair localizes on the less electronegative atom. The A−B bonding 1π orbitals of heterodiatomics have a higher amplitude on the more electronegative atom B, whereas the antibonding 2π orbitals (LUMO) show larger contributions on the more electropositive atom A. The LUMOs 2π decrease by approximately 1 eV in energy along the series of the first-row diatomics NN, CO, and BF.

For CO and BF, MOs 3σ and 4σ should be more localized on the more electronegative atom B and the HOMO 5σ is expected to show a substantial weight on the less electronegative atom A. We do observe these trends across the series NN, CO, and BF. Molecular orbital 4σ comes down to lower energy, while the HOMO 5σ rises and is more localized on the electropositive atom as we go from N_2 (50%) to CO (90%) to BF (98%).

(20) Pauling, L. *The Chemical Bond−A Brief Introduction to Modern Structural Chemistry*; Cornell University Press: Ithaca, NY, 1967; Chapter 7.

(21) (a) Radzig, A. A.; Smirnov, B. M. *Reference Data on Atoms, Molecules, and Ions*; Springer-Verlag: Berlin, 1985; Chapter 10, 15.1. (b) Herzberg, G.; Huber, K. P. *Molecular Spectra and Molecular Structure. IV. Constants of Diatomic Molecules*; Van Nostrand: Princeton, NJ, 1979. (c) Klemperer, W. *Annu. Rev. Phys. Chem.* **1995**, 46, 1. (d) Lovas, F. J.; Johnson, D. R. *J. Chem. Phys.* **1971**, 55, 41. (e) Ransil, B. J. *Rev. Mod. Phys.* **1960**, 32, 245.

(22) Allen's electronegativities χ are 1.916 (Si), 2.051 (B), 2.544 (C), 3.066 (N), 3.610 (O), and 4.193 (F): Allen, L. C. *J. Am. Chem. Soc.* **1989**, *111*, 9003.

(23) (a) Hoffmann, R. *Acc. Chem. Res* **1971**, *4*, 1. (b) Jorgensen, W. L.; Salem, L. *The Organic Chemist's Book of Orbitals*; Academic Press: New York, 1973; Chapter I.20. (c) Heilbronner, E.; Bock, H. *Das HMO-Modell und seine Anwendung*; Verlag Chemie: Weinheim, Germany, 1968.

Scheme 1

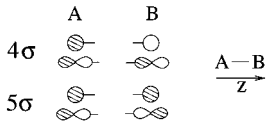

The s and p_z components leading to the shape of the σ valence orbitals 4σ and 5σ of N_2 are graphically indicated in Scheme 1.

An approach to understanding how the character of the 5σ HOMO changes as one progresses along N_2, CO, and BF is to look how the zeroth order picture of mixing develops. In N_2, the 5σ derives mainly from $2p_z(A) - 2p_z(B)$, i.e. an A−B bonding combination. One could use this picture as a starting point for describing the 5σ in CO and BF, too, as we did above. However, another perspective recognizes that the character of the 5σ HOMO shifts more and more toward $2s(A) - 2p_z(B)$, i.e. "initially" A−B antibonding, with a bonding admixture of $2p_z(A)$. Of course, both approaches arrive ultimately at the same result.

It is interesting to estimate the bonding or antibonding character for the 5σ orbitals of the four diatomics. The Mulliken overlap population of an MO for a certain bond, normalized for 1 electron, i.e. $\sum c_i c_j S_{ij}$, is a measure of this character (c_i, c_j = coefficients of AOs on atom A and B, respectively; S_{ij} = corresponding overlap matrix element). We calculate small negative numbers (for 1 electron) for all diatomic 5σ orbitals: −0.12 (CO), −0.09 (BF) −0.06 (SiO), −0.03 (N_2). For comparison, the corresponding overlap populations (for 1 electron) of the antibonding 2π orbitals are −0.35, −0.17, −0.14, and −0.44. Thus, judging from these numbers, the 5σ MOs are slightly antibonding, close to nonbonding. This is not a new result; the antibonding nature of 5σ(CO) was discussed by Graham and by Hall and Fenske[24] over 25 years ago.

Why the slight antibonding in 5σ? As shown for N_2 in Scheme 1, the 5σ MOs are made up from a combination of $p_z(A)$ and $p_z(B)$ orbitals that is bonding and a bonding combination of s(A) and s(B) as well. But AOs $p_z(A)$ and s(B) (as well as $p_z(B)$ and s(A) by symmetry) are mixed in in an antibonding fashion. The s−s overlap values computed for N_2 are approximately of the same magnitude as the s−p overlaps, whereas the p_z-p_z overlaps are actually much smaller in the range of distances near the equilibrium separation. Therefore, the bonding gained due to s−s and p−p overlap in $5\sigma(N_2)$ is counterbalanced by s−p_z interaction, and $5\sigma(N_2)$ emerges slightly net antibonding. For the heterodiatomics, the dominant factor for evaluating the bonding character of 5σ is the s(A)−p_z(B) overlap, and we obtain slight antibonding character for these molecular orbitals as well.

B. SiO and the Other Diatomics. The bonding in SiO is quite distinctive, especially if we compare it to its homologue CO (Figure 2; see also Table 5 in the Supporting Information). Generally, the energy differences of atomic orbitals of the same type in A (=C, Si) and B (=O) are larger for SiO. The $\langle 2p_\pi|2p_\pi\rangle$ overlap of 0.27 is significantly lower than that in CO (0.35) and N_2 (0.37). Together, these factors make the π bond in SiO ($\Delta E(\pi) = -66.9$ kcal/mol) considerably weaker than in CO (−185.8 kcal/mol). A consequence is a much smaller π/π^* level splitting in SiO. We end up with an 1π(SiO) that is relatively high in energy (3.8 eV above 1π(CO)) and a low-lying 2π(SiO) orbital (actually lower in energy than that of BF).

The nature of the SiO HOMO 5σ has changed, in comparison to the other diatomics. MO 5σ(SiO) seems to follow the general trend of being higher in energy as the difference in electronegativity increases (see Figure 2). On the other hand, MO 4σ(SiO) is also very high in energy, in fact much higher in energy than its counterparts in CO and BF. This 4σ(AB) orbital generally moves to lower energy as the difference in electronegativity is increased. An interaction diagram for SiO (not shown here) reveals that the 3s(Si) AO matches very well in energy the $2p_z(O)$. MO 3σ(SiO) is mainly formed by 2s(O), and the main interaction building up 4σ and 5σ is between 3s(Si) and $2p_z(O)$. Furthermore, the interaction between Si and O orbitals in SiO is much weaker than for C and O in CO. We calculate a smaller $\langle 2s(A)|2p_z(B)\rangle$ overlap for SiO (0.28) in comparison to CO (0.39) and a total σ orbital interaction energy $\Delta E(\sigma)$ of 493.0 kcal/mol for SiO in comparison to 717.6 kcal/mol for CO. As a consequence of this difference, MO 4σ(SiO) lies relatively high in energy. The main contributions to 4σ(SiO) are 56% 3s(Si) and 31% $2p_z(O)$, and to 5σ(SiO) 27% are 3s(Si), 21% $3p_z(Si)$, and 49% $2p_z(O)$. AO $3p_z(Si)$ mixes in significantly in 5σ(SiO), but this MO is much less weighted on the eventual metal coordinating atom than in CO or BF.

A frontier-orbital approach to donor and acceptor capabilities of ligands leads us to consider molecules with occupied orbitals high in energy as the better donors and molecules with low-lying unoccupied orbitals as the better acceptors. Another criterion for coordinating capability is the localization of an orbital within the molecule, i.e., whether it is highly localized on the coordinating atom or not. Therefore, we conclude from the discussion above that CO is a "better" ligand than N_2. And we are led to think that BF is a molecule with similar or possibly even better σ-donor and π-acceptor qualities as compared with CO. But it is difficult to predict ligating properties for SiO within this scheme, only considering MOs 5σ(SiO) and 2π(SiO). In comparison to CO, we might expect comparable σ bonding and better π back-bonding, but we have to take the high-lying MOs 4σ(SiO) and 1π(SiO) into account.

4. Geometries, Bond Enthalpies, and Frequencies of A−B, $Fe(CO)_4AB$, and $Fe(AB)_5$

In this section we discuss the optimized geometries, calculated bond dissociation enthalpies and some computed frequencies for the complexes $Fe(CO)_4AB$ (**1** and **2**) and $Fe(AB)_5$ (**3**). The computed results are assembled in Table 1. The $M(AB)_5$ system was chosen in preference to a d^6 $M(AB)_6$ just because it offers the potential of differential bonding in axial and equatorial sites.

A. Geometries and Frequencies. The geometries of the iron complexes were optimized within C_{3v} symmetry restriction for **1**, under C_{2v} symmetry for **2**, and D_{3h} symmetry for **3**. Vibrational analyses for all optimized geometries demonstrate that they are all energy minima at the level of theory applied here. For $Fe(AB)_5$ (**3a**−**d**) we obtained ideal trigonal bipyramidal geometries, the distances between the central atom iron and the coordinated atom A of the diatomic molecules being 1.85 Å (axial) and 1.87 Å (equatorial) for Fe−N in **3a**, 1.81 Å for Fe−C in **3b** (for both axial and equatorial ligands), 1.78 Å (both distances) for Fe−B in **3c**, and 2.12 Å (again both distances) for Fe−Si in **3d**. Further details of the optimized geometries are provided in the Supporting Information.

There is only one X-ray crystal structure known experimentally for complexes of the type **3**, namely for $Fe(CO)_5$ (**3b**).[25] This structure has been reinvestigated recently by Braga, Grepioni, and Orpen.[25a] The Fe−C distances were found in their study to be 1.801(3) and 1.804(2) Å for the equatorial

(24) (a) Graham, W. A. G. *Inorg. Chem.* **1968**, *7*, 315. (b) Hall, M. B.; Fenske, R. F. *Inorg. Chem.* **1972**, *11*, 768.

Table 1. Selected Bond Lengths d(AB) and d(FeA) (Å),[a] Bond Angles $C_{ax}-Fe-A$ and $C_{eq}-Fe-A$ (deg), Bond Dissociation Enthalpies BDE $= -\Delta H_{298}$ (kcal/mol),[b] and Frequencies ν (cm^{-1}) of **1**−**3**[c]

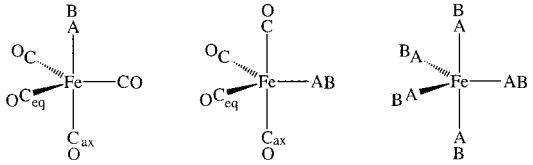

1 **2** **3**

sym	L	d(AB)	d(FeA)	$C_{ax}-Fe-A$	$C_{eq}-Fe-A$	$\Delta H = -$BDE	ν
C_{3v}	**1a** (NN)	1.11	1.88	180.0	91.2	−18.1	1982 (e), 1998, 2056, 2224 (a_1)
	1b (CO)	1.15	1.81	180.0	90.0	−42.3	1989 (e′), 2003 (a_2'')[d]
	1c (BF)	1.27	1.81	180.0	86.7	−67.9	1977 (e), 1490, 2000, 2058 (a_1)
	1d (SiO)	1.53	2.17	180.0	89.2	−35.6	1989 (e), 1205, 2008, 2066 (a_1)
C_{2v}	**2a** (NN)	1.11	1.89	93.3	117.6	−19.0	1993, 2064, 2211 (a_1), 1996 (b_1), 1978 (b_2)
	2b (CO)	1.15	1.81	90.0	120.0	−42.3	1989 (e′), 2003 (a_2'')[d]
	2c (BF)	1.28	1.80	81.7	123.4	−66.7	1460, 1995, 2059 (a_1), 1979 (b_1), 1992 (b_2)
	2d (SiO)	1.54	2.16	88.1	119.8	−39.7	1197, 2011, 2073 (a_1), 2001 (b_1), 2002 (b_2)
D_{3h}	**3a** (NN)	1.12	1.85 (ax), 1.87 (eq)	angles $A_{eq}-M-A_{eq}$		−34.0	2144 (e′), 2173 (a_2'')
	3b (CO)	1.15	1.81	120°;		−56.5	1989 (e′), 2003 (a_2'')
	3c (BF)	1.29	1.78	angles $A_{eq}-M-A_{ax}$		−75.2	1415 (e′), 1432 (a_2'')
	3d (SiO)	1.53	2.12	90°		−52.6	1204 (e′), 1206 (a_2'')

[a] NL-SCF/TZ(2P). [b] ΔH for **1** and **2** corresponds to the bond enthalpy $\Delta H(Fe(CO)_4AB \rightarrow Fe(CO)_4 + AB)$ and for **3** to the mean bond enthalpy $\Delta H(Fe(AB)_5 \rightarrow Fe + 5AB)/5$. [c] LDA/TZ(2P). [d] In D_{3h} symmetry.

Fe−C bonds and 1.811(2) Å for the bonds to the axial carbonyl groups.[26] Interestingly, in the most recent gas-phase electron-diffraction study[25d] the average equatorial Fe−C distance was found to be *longer* than the axial values (1.827(3) vs 1.807(3) Å). We have obtained Fe−C distances of 1.811 (eq) and 1.812 Å (ax) for **3b**. We do not really want to enter the discussion as to which experimental structure determination is better; it is clear that the difference between equatorial and axial CO ligands is not very large and that the computed Fe−C distances are in good agreement with the experiment.

Compounds $Fe(CO)_4AB$ (**1** and **2**) optimize to distorted trigonal bipyramidal complexes with small deviations from their idealized structure. As may be seen in Table 1, especially the $C_{eq}-M-A$ angles for **1** and $C_{ax}-M-A$ for **2** deviate from 90°. For the dinitrogen compounds $Fe(CO)_4(N_2)$ (**1a** and **2a**) we obtain geometries where these angles are enlarged, while for the BF and SiO complexes **1c**,**d** and **2c**,**d** we compute angles smaller than 90°.

The structures of **1a** and **2a** (AB = N_2) as well as **1c** and **2c** (AB = BF) are very close in energy, 0.9 and 1.2 kcal/mol, respectively. For $Fe(CO)_4(SiO)$ we calculate a more significant energy difference of 4.1 kcal/mol between the C_{3v} structure **1d** and its C_{2v} analogue **2d**. In the case of the N_2 and SiO complexes $Fe(CO)_4AB$ we obtain the overall energy minimum structure for the C_{2v} geometries **2a**,**d**; for AB = BF the C_{3v} structure **1c** is favored by 1.2 kcal/mol.

We want to compare these results with earlier qualitative ideas on donor/acceptor substitution patterns in trigonal bipyramidal d^8 $M(AB)_5$ complexes,[27] where an argument was given for the fact that stronger σ donors prefer the axial position and cylindrical π acceptor ligands the equatorial site. This idea holds for AB = N_2 and BF: the (arguably) weaker (N_2) donor in comparison to CO preferentially occupies the equatorial site; the better donor (BF), the axial position. For SiO we calculate a strong preference for the equatorial site, which suggests (on the basis of these qualitative ideas) that SiO should be either a better π acceptor or a worse σ donor than CO (or both). The result unfortunately disagrees with the general characterization of the ligand's bonding capabilities outlined below but reflects a change in bonding as we go from SiO to CO. We will explain this finding in more detail later.

The lengthening of the A−B multiple bond in transition metal complexes L_nM-A-B is usually taken as evidence for back-bonding, that is electron transfer from the metal to the π^* orbital of AB.[3] For all complexes **1**−**3** the A−B distances differ only slightly for the free and the ligated diatomic—the largest elongation being approximately 0.02 Å. However, this increase is not observed for Si−O complexes **1b** and **2b**, where the Si−O distance remains almost constant upon ligation.

Differences in the electronic structure are probably better identified by looking at the changes of the frequencies between the free and complexed molecule AB. For the N_2 complexes **1a**, **2a**, and **3a** and the CO complex **3b**, the A−B stretch frequencies decrease, as experimentally observed. Interestingly, we calculate a shift to higher frequencies for the BF and SiO ligands in **c**/**d** of **1**−**3** compared to their calculated values for the free molecule, for example 1415 and 1432 cm^{-1} in **3c** as compared with 1380 cm^{-1} in the free ligand. This result supports the general conclusion of our discussion on A−B bonding that both 5σ(SiO) and 5σ(BF) are at first-order combinations of 2s atomic orbitals; that is, they are A−B antibonding. Charge transfer from the 5σ(AB) orbital to the $Fe(CO)_4$ fragment decreases the population of this orbital and increases AB bonding. We will discuss this point in more detail below.

B. Side-On Bonded Isomers. A rare type of binding by molecular nitrogen is the side-on mode. Side-bonded η^2

(25) (a) Braga, D.; Grepioni, F.; Orpen, A. G. *Organometallics* **1993**, *12*, 1481. (b) Hanson, A. W. *Acta Crystallogr.* **1962**, *15*, 930. (c) Donohue, J.; Caron, A. *Acta Crystallogr.* **1964**, *17*, 663. (d) Hedberg, L.; Iijima, T.; Hedberg, K. *J. Chem. Phys.* **1979**, *70*, 3224.

(26) We want to emphasize here the reservations one must have in interpreting experimental data (the differences in the bond length described in the solid-state structure are approximately 0.01 Å) obtained from X-ray crystal structure analyses of organometallic compounds. In an important study by G. Orpen and co-worker the chemical limitation on the reliability of results obtained from X-ray crystal data was demonstrated. These authors suggest an inherent standard deviation in metal−ligand bond lengths (due to packing, not the accuracy of crystallographic structure refinement) that usually lies between 0.01 and 0.02 Å: Martín, A.; Orpen, A. G. *J. Am. Chem. Soc.* **1996**, *118*, 1464.

(27) Rossi, A. R.; Hoffmann, R. *Inorg. Chem.* **1975**, *14*, 365.

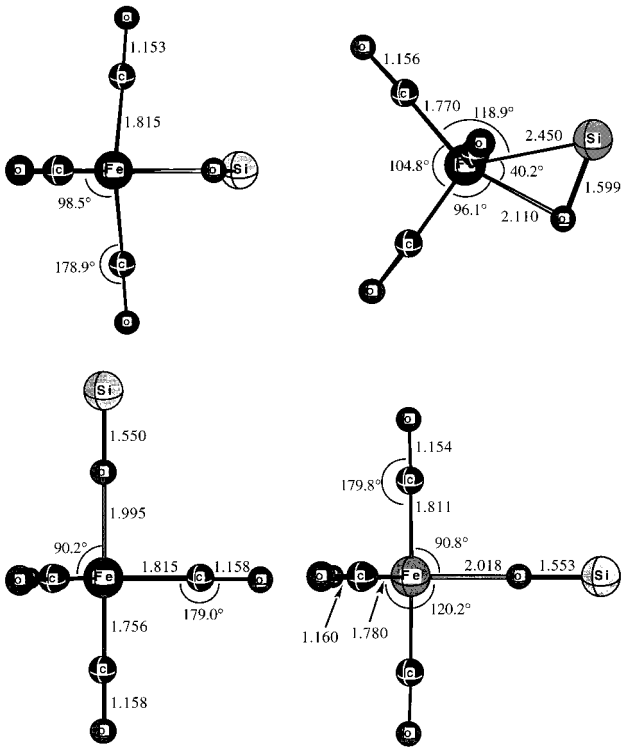

Figure 3. Optimized geometries of $Fe(CO)_4(\eta^2\text{-SiO})$ (top, left and right) and $Fe(CO)_4(OSi)$, C_{3v} (bottom, left), C_{2v} (bottom, right).

nitrogen ligands have been proposed to be present for example in dinuclear nickel complexes,[28a] in $Cp_2Zr(CH_2SiMe_3)(\eta^2\text{-}N_2)$,[28b] and in matrix-isolated $Co(\eta^2\text{-}N_2)$.[28c] This mode is a reasonable intermediate in a possible end to end rotation of terminal bound nitrogen atoms.[28d] Crystallographically characterized are an unusual dinuclear samarium complex $[Cp^*_2Sm]_2(\mu\text{-}\eta^2\text{:}\eta^2\text{-}N_2)$[28e] as well as a dinuclear zirconium complex $\{[(R_2PCH_2SiMe_2)_2N]\text{-}ZrCl\}_2(\mu\text{-}\eta^2\text{:}\eta^2\text{-}N_2)$.[28f,g] In the course of our investigation we were led to consider the η^2 or even end-on coordination mode of the AB ligand *via its B atom* to the $Fe(CO)_4$ fragment. Especially for SiO, with its 1π orbitals relatively high in energy and its large orbital amplitude on oxygen in 4σ and 5σ MOs, these possibilities are intriguing. As a matter of fact, we did find minima for C_{3v} and C_{2v} oxygen-bound complexes of the type $Fe(CO)_4OSi$, 19.0 (C_{3v}, axial substitution) and 23.4 kcal/mol (C_{2v}, equatorial substitution) higher in energy than calculated for the silicon-bound isomers **1d** and **2d**. Furthermore, we found a very interesting side-on coordinated, C_s symmetrical isomer $Fe(CO)_4(\eta^2\text{-SiO})$, only 12.7 kcal/mol higher in energy than the overall minimum structure C_{2v}-$Fe(CO)_4SiO$ (**2d**). The optimized geometries of these isomers are shown in Figure 3.

C. Bond Dissociation Enthalpies. The bond dissociation enthalpies ($BDE = -\Delta H_{298}$) listed in Table 1 are derived from bonding energies (BE) after thermal corrections (see section 2A). The BDE's for **3** are averaged with respect to the dissociation of $Fe(AB)_5$ into Fe and 5 AB, to obtain results for one Fe−AB bond; those for **1** and **2** are given with respect to dissociation of $Fe(CO)_4AB$ into the fragments $Fe(CO)_4$ and AB. In general, this dissociation enthalpy can be obtained from the bonding energy expressed as

$$BE = E([M]-AB) - E([M]) - E(AB) \qquad (5)$$

where $E([M]-AB)$ is the energy of the equilibrium structure of the complex [M]−AB; $E([M])$ and $E(AB)$ are generally the ground-state energies of the complex fragment [M] and the free ligand AB.

In their work on the structure and reactions of matrix-isolated iron tetracarbonyl, Poliakoff and Turner[10] suggested—based on extended Hückel calculations of Burdett et al.[29a]—for $Fe(CO)_4$ a C_{2v} triplet ground state with angles α and β (see Table 2) of approximately 130 and 115°. Various other groups have later investigated the ground state of $Fe(CO)_4$, using ab initio and DFT methods.[30]

To have a good reference for the dissociation energies of the C_{2v} and C_{3v} complexes shown in Table 2, we have examined several possible geometries for the triplet and singlet state of $Fe(CO)_4$. The results are summarized in Table 2.

We find a $^3B_2$ ground state for $Fe(CO)_4$, of C_{2v} geometry ($\alpha = 148.8°$ and $\beta = 97.2°$). The lowest energy singlet state (^1A) with a C_{3v} structure—a possible intermediate during the dissociation of an axial carbon monoxide from $Fe(CO)_5$—is in our calculation 6.7 kcal/mol higher in energy. With respect to its triplet ground state, the thermal dissociation

$$Fe(CO)_4AB \rightarrow Fe(CO)_4 + AB \qquad (6)$$

is a spin-forbidden process, but our calculations show that there is an appropriate $^1A_1$ state very close in energy, only 0.6 kcal/mol higher than the $^3B_2$ ground state of $Fe(CO)_4$. Throughout this paper, bond dissociation enthalpies are given with respect to the triplet ground state of $Fe(CO)_4$.

For $Fe(CO)_5$ the first dissociation enthalpy of 42.3 kcal/mol obtained by this method is in good agreement with the experimentally observed value of 41 ± 2 kcal/mol.[31] The dissociation enthalpies obtained for the N_2 complexes **1a** and

Table 2. Optimized Geometries of $^3B_2$ C_{2v}, $^1A_1$ C_{2v}, and $^1A_1$ C_{3v} $Fe(CO)_4$ and Computed Energies Relative to the $^3B_2$ C_{2v} Ground State of $Fe(CO)_4$[a]

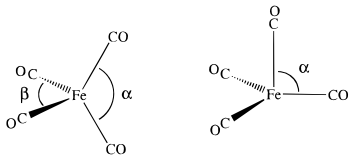

C_{2v} **C_{3v}**

	C_{2v} $^3B_2$	C_{2v} $^1A_1$	C_{3v} $^1A_1$
α (deg)	148.8	164.3	90.8
β (deg)	97.2	128.7	
E_{rel} (kcal/mol)	0.00	0.62	6.65

[a] NL-SCF/TZ(2P).

(28) (a) Jones, K.; Brauer, D. J.; Krüger, C. Roberts, P. J.; Isay, Y.-H. *J. Am. Chem. Soc.* **1976**, *98*, 74. (b) Jefferey, J.; Lappert, M. F.; Riley, P. I. *J. Organomet. Chem.* **1979**, *181*, 25. (c) Ozin, G. A.; Vander Voet, A. *Can. J. Chem.* **1973**, *51*, 637. (d) Cusanelli, A.; Sutton, D. *J. Chem. Soc., Chem. Commun.* **1989**, 1719. (e) Evans, W. J.; Ulibarri, T. A.; Ziller, J. W. *J. Am. Chem. Soc.* **1988**, *110*, 6877. (f) Fryzuk, M. D.; Haddad, T. S.; Rettig, S. J. *J. Am. Chem. Soc.* **1990**, *112*, 8185. (g) Fryzuk, M. D.; Haddad, T. S.; Mylvaganam, M.; McConville, D. H.; Rettig, S. J. *J. Am. Chem. Soc.* **1993**, *115*, 2782.

(29) (a) Burdett, J. K. *J. Chem Soc., Faraday Trans. 2* **1974**, *70*, 1599. (b) Elian, M.; Hoffmann, R. *Inorg. Chem.* **1975**, *14*, 1058.

(30) Theoretical work on $FeCO_4$: (a) Daniel, C.; Bénard, M.; Dedieu, A.; Wiest, R.; Veillard, A. *J. Phys. Chem.* **1984**, *88*, 4805. (b) Ziegler, T.; Tschinke, V.; Fan, L. Becke, A. D. *J. Am. Chem. Soc.* **1989**, *111*, 9177. (c) Lyne, P. D.; Mingos, D. M. P.; Ziegler, T.; Downs, A. J. *Inorg. Chem.* **1993**, *32*, 4785. (d) Barnes, L. A.; Rosi, M.; Bauschlicher, C. W., Jr. *J. Chem. Phys.* **1991**, *94*, 2031. Experimental work on $Fe(CO)_4$: (e) Original work; see ref 10. (f) Barton, T. J.; Grinter, R.; Thomson, A. J.; Davis, B.; Poliakoff, M. *J. Chem. Soc., Chem. Commun.* **1977**, 841. (g) Poliakoff, M.; Weitz, E. *Acc. Chem. Res.* **1987**, *20*, 408. (h) Ouderdirk, A. J.; Werner, P.; Schultz, N. L.; Weitz, E. *J. Am. Chem. Soc.* **1983**, *105*, 3354. (i) Seder, T. A.; Ouderdirk, A. J.; Weitz, E. *J. Chem. Phys.* **1986**, *85*, 1977.

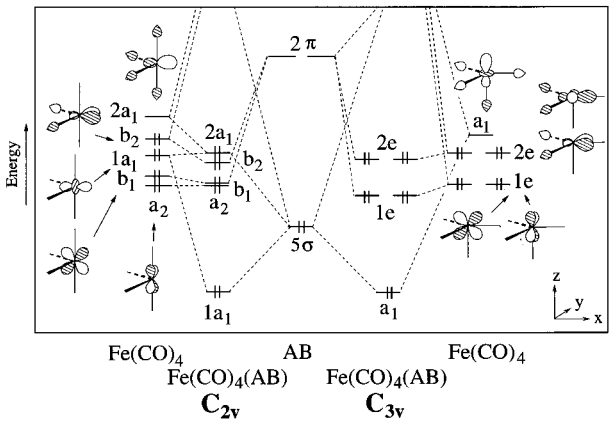

Figure 4. Schematic FMO diagrams of C_{2v}- (left side) and C_{3v}-Fe(CO)$_4$−AB (right side), built up from Fe(CO)$_4$ fragments and a σ donor, π acceptor ligand AB.

2a are 18.1 and 19.0 kcal/mol, indicating the relative thermal instability of these compounds with respect to this dissociation. Interestingly, the calculated dissociation enthalpies for the SiO complexes **1d** and **2d** are with 35.6 and 39.7 kcal/mol similar to those of Fe(CO)$_5$, whereas the boron fluoride compounds **1c** and **2c** have the highest binding energy observed in this series (approximately 67 kcal/mol for the Fe(CO)$_4$(BF) systems). There is no question that BF complexes are thermodynamically stable.

These results suggest ligation properties (i.e. the complex fragment−ligand bond strength) in the order N_2 < CO, SiO < BF, an order confirmed by the values obtained for an average bond energy for the compounds Fe(AB)$_5$ (**3**). Table 1 shows the enthalpies for the dissociation of Fe(AB)$_5$ in Fe and 5 ligands AB, averaged for one bond. We calculate averaged values of 34.0 (N_2), 52.6 (SiO), 56.5 (CO), and 75.2 kcal/mol (BF), respectively.

5. Bonding in Fe(CO)$_4$AB and Fe(AB)$_5$

The dissociation enthalpies of **1**−**3** discussed above indicate an increasing Fe−AB bond strength across the series N_2, CO, and BF. The Fe−Si bond strengths in **1d**, **2d**, and **3d** are surprisingly similar to those of carbonyl compounds. We next describe the Fe(CO)$_4$−AB bonding in some detail. The fragment molecular orbital (FMO) diagrams of C_{2v}- and C_{3v}-Fe(CO)$_4$−AB built up from Fe(CO)$_4$ fragments and an AB ligand are quite familiar;[29b,30c,e,32] such FMO diagrams between a C_{2v}- and a C_{3v}-Fe(CO)$_4$ fragment and a σ donor, π acceptor ligand AB are schematically shown in Figure 4.

Before the Fe(CO)$_4$−AB bonding is analyzed, it is relevant to recall the electronic structure of the Fe(CO)$_4$ group and its bonding capabilities in the two fragment geometries. Among the frontier orbitals of C_{2v}-Fe(CO)$_4$ (left side of Figure 4) we distinguish the relatively low-lying a_2, b_1, and $1a_1$ orbitals that are metal centered and d_{yz}, d_{xz}, and "d_{x^2}" in character. These orbitals are involved in some back-bonding with the equatorial and axial carbonyls of the Fe(CO)$_4$ unit (not shown in our orbital drawings). Higher in energy are the orbitals b_2 (HOMO) and $2a_1$ (LUMO). The former is mainly d_{xy} in character with some p_y contribution. This occupied fragment orbital is suitable for π-donation toward an incoming π-acceptor orbital of AB at the empty coordination site. The $2a_1$ orbital is a dsp hybrid with considerable ligand (CO) character. This orbital, pointing toward the empty coordination side, is a good σ-acceptor orbital.

Scheme 2

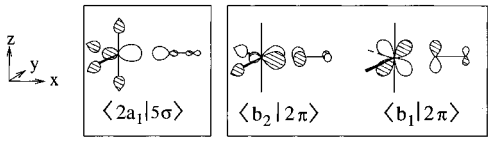

Scheme 3

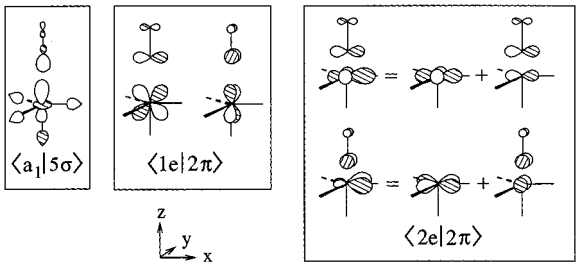

In the interaction of C_{2v}-Fe(CO)$_4$ with AB these a_1 and b_2 interactions are mainly responsible for the binding of the ligand to the metal fragment. There is some π-back-bonding between the π^*_z AB orbital and Fe(CO)$_4$ b_1 and also σ-interactions between lower lying Fe(CO)$_4$ orbitals and σ AB orbitals, especially between $1a_1$ and 5σ AB. The main interactions are summarized in Scheme 2 above.

The orbitals of a C_{3v} Fe(CO)$_4$ unit are also well-known.[32] At low energy lies the 1e, which is primarily metal d_{xz} and d_{yz}, stabilized by back-bonding to carbonyl π^* orbitals of the (CO)$_4$ fragment (not shown in detail in the orbital sketch). At higher energy is the 2e. These orbitals are mainly $d_{x^2-y^2}$ and d_{xy}, hybridized with metal p_x and p_y. Some carbonyl σ is mixed in in an antibonding fashion, as well as some carbonyl π^* character. Finally, the a_1 LUMO is mainly d_{z^2} in character. Contributions of metal s and p_z hybridize this orbital away from the ligands, and carbonyl σ is mixed into a_1 antibonding with respect to d_{z^2}. In the interaction of C_{3v} Fe(CO)$_4$ with AB, the main bonding contributions are the donation from the AB σ orbitals to a_1 and the back-bonding of 1e and 2e to the AB π^* orbitals 2π. These crucial interactions are shown in Scheme 3 in detail.

For a full description of the back-bonding we need to consider in some detail the interaction of 2e of the metal fragment and 2π of AB. We calculate a large Fe 4p contribution to orbital 2e (13% p_x or p_y, respectively). These atomic orbitals have—as shown in Scheme 3—significant overlap with the 2π orbitals of the AB unit. The admixture of Fe 4p in 2e is crucial for the back-donation of this fragment orbital to AB, and—as we will see later—the fragment orbital overlaps $\langle 2e|2\pi\rangle$ are actually larger than $\langle 1e|2\pi\rangle$.

The energy decomposition, important fragment orbital overlaps, and Fe(CO)$_4$ and AB fragment orbital populations for the Fe(CO)$_4$−AB bonding in compounds **1a**−**d** (C_{3v}) and **2a**−**d** (C_{2v}) are given in Table 3.

A. Bonding of N_2, CO, and BF to Fe(CO)$_4$. The total bond dissociation enthalpy (BDE) of C_{2v}- and C_{3v}-Fe(CO)$_4$−AB increases as we go from N_2 to CO to BF. As the decomposition of the orbital interaction energy in Table 3 shows, this is the result of both stronger σ- ($\Delta E(a_1)$) and stronger π-bonding ($\Delta E(b_1) + \Delta E(b_2)$ or $\Delta E(e)$) between the Fe(CO)$_4$ fragment

(31) Lewis, K. E.; Golden, D. M.; Smith, G. P. *J. Am. Chem. Soc.* **1984**, *106*, 3905.

(32) (a) Albright, T. A.; Burdett, J. K.; Whangbo, M.-H. *Orbital Interactions in Chemistry*; Wiley: New York, 1985; Chapters 17 and 19. (b) Bersucker, I. B. *Electronic Structure and Properties of Transition Metal Compounds*; Wiley: New York, 1996; pp 217−267 and references therein.

Table 3. Analysis of the $Fe(CO)_4$−AB Bonding in C_{3v}- and C_{2v}-$Fe(CO)_4AB$ (AB = N_2, CO, BF, and SiO)[a]

	C_{3v}-$Fe(CO)_4$ (**1a**−**d**)				C_{2v}-$Fe(CO)_4$ (**2a**−**d**)			
L	NN	CO	BF	SiO	NN	CO	BF	SiO
				Energy Decomposition (kcal/mol)[b]				
$\Delta E(a_1)$	−26.9	−45.8	−80.4	−58.7	−26.0	−42.0	−78.7	−48.7
$\Delta E(e)$, $\Delta E(b_1 + b_2)$[c]	−26.6	−42.8	−46.5	−31.7	−27.0	−45.6	−53.7	−34.0
ΔE_{oi}	−53.5	−88.6	−126.9	−90.4	−53.0	−87.6	−132.4	−82.7
$\Delta E°$	25.3	35.0	46.9	44.5	28.1	37.7	54.7	37.5
$\Delta H_{298} = -BDE$	−18.1	−42.3	−67.9	−35.6	−19.0	−42.3	−66.7	−39.7
				Fragment Orbital Overlaps				
$\lvert\langle a_1\rvert 5\sigma\rangle\rvert$, $\lvert\langle 2a_1\rvert 5\sigma\rangle\rvert$[c]	0.27	0.43	0.48	0.33	0.27	0.43	0.50	0.35
$\lvert\langle a_1\rvert 4\sigma\rangle\rvert$, $\lvert\langle 2a_1\rvert 4\sigma\rangle\rvert$[c]	0.25	0.16	0.09	0.32	0.25	0.16	0.10	0.34
$\lvert\langle 1e_1\rvert 2\pi\rangle\rvert$, $\lvert\langle b_1\rvert 2\pi\rangle\rvert$[c]	0.09	0.13	0.14	0.12	0.12	0.16	0.09	0.15
$\lvert\langle 2e_1\rvert 2\pi\rangle\rvert$, $\lvert\langle b_2\rvert 2\pi\rangle\rvert$[c]	0.11	0.17	0.21	0.20	0.16	0.26	0.32	0.29
				Fragment Orbital Population (e)				
$5\sigma(a_1)$	1.73	1.53	1.13	1.36	1.75	1.55	1.02	1.40
2π(e), $2\pi(b_1)$[c]	0.13	0.21	0.25	0.22	0.11	0.14	0.17	0.15
$2\pi(b_2)$[d]					0.19	0.27	0.37	0.29

[a] NL-SCF/TZ(2P). [b] See section 2B. [c] Entry for C_{3v}, C_{2v}-$Fe(CO)_4AB$. [d] Entry for C_{2v}-$Fe(CO)_4AB$.

and the ligand AB. For the C_{2v} compounds **2a**−**c** we calculate, for example, −26.0 kcal/mol (N_2), −42.0 kcal/mol (CO), and −78.7 kcal/mol (BF) due to σ interactions and −37.0 kcal/mol (N_2), −45.6 kcal/mol (CO), and −53.7 kcal/mol (BF) due to π interactions. The stronger σ bonding interaction is mainly the result of better fragment orbital overlaps between 5σ (AB) and $2a_1$ ($Fe(CO)_4$, C_{2v}) and a_1 ($Fe(CO)_4$, C_{3v}). The 5σ(AB) orbitals moreover have a better energy match with $a_1/2a_1$ as they increase in energy. This finding is in accord with the trends discussed above for the ligands AB.

BF with its high-lying 5σ MO is the best σ-donating ligand in this series. This view is supported by the fragment orbital populations shown in Table 3. The 5σ(AB) orbital is for example depopulated by 0.27/0.25 (C_{3v}/C_{2v} structure) electrons in the case of $Fe(CO)_4NN$, by 0.47/0.43 electrons for $Fe(CO)_4$−CO, and by 0.96/0.98 electrons for $Fe(CO)_4$−BF.

For π back-bonding, we predicted an increasing interaction in the same order, namely BF > CO > N_2 due to the increasing localization of 2π(AB) on the more electropositive atom A. As Table 3 shows, this trend is observed but not as well-developed as for the σ-type interaction discussed above. The overlap of 2π(AB) with the metal orbitals of appropriate symmetry increases only little as we go from N_2 to CO to BF; so does the electron transfer from the $Fe(CO)_4$ fragment to AB.

The $Fe(CO)_4$−AB bonding pictures differ somewhat as far as their σ and π components go, as the difference in electronegativity within the diatomic increases. Both σ and π interactions are relatively small for AB = N_2, and σ and π contributions are surprisingly well balanced. The π contribution to iron−dinitrogen bonding for C_{2v}-$Fe(CO)_4N_2$ (**2a**) is actually slightly larger than the σ contribution to the net orbital interaction energy. As the AB ligand becomes more polar, σ bonding grows more important. For AB = CO the overall interaction between $Fe(CO)_4$ and the diatomic ligand is much stronger, but the σ and π contributions are still balanced. Thus we calculate for example −45.8 kcal/mol (σ) and −42.8 kcal/mol (π) for the C_{3v} fragment compound **1b** and −42.0 (σ) and −45.6 kcal/mol (π) for the C_{2v} fragment complex **2b**. Note how important π back-donation is for both N_2 and CO ligands as we interact them with the $Fe(CO)_4$ fragments. It makes up approximately half of the orbital interaction energy!

Both the high σ orbital interaction energy (in comparison to N_2) and the excellent π-accepting capabilities make CO the superb ligand that it is in organometallic chemistry. The highly dipolar BF, on the other hand, emerges in our calculations as the best ligand in terms of bonding energies. The increase in bonding energy—approximately 25 kcal/mol for the $Fe(CO)_4$−AB bond (BF, compared with CO)—is mainly due to the better σ-donating abilities computed for the BF ligand.

B. The SiO Ligand Coordinated to $Fe(CO)_4$. What about the bonding capabilities of SiO? The SiO-containing **1d** and **2d** are probably best compared to complexes of their homologous CO compounds **1b** and **2b**. We calculate for the $Fe(CO)_4$−SiO bond in **1d** and **2d** orbital interaction energies similar to those of $Fe(CO)_4$−CO (**1b**, **2b**). The energy decomposition of the orbital interactions in Table 3 shows the SiO σ-bonding energy $\Delta E(a_1)$ of −58.7 kcal/mol (C_{3v}) and −48.7 kcal/mol (C_{2v}) is higher, whereas ΔE(e) (−31.7 kcal/mol) and $\Delta E(b_1) + \Delta E(b_2)$ (−34.0 kcal/mol) are lower than the bonding energies of the equivalent CO complexes. This result indicates a weaker π-bonding interaction for the silicon monoxide complexes. In terms of σ-donating and π-accepting capabilities, the bonding energy decomposition scheme of Table 3 suggests that SiO is as a σ donor better than CO and as a π acceptor ligand comparable to N_2 rather than to CO.

The bonding situation thus changes as we go from the second group diatomic CO to its higher homologue SiO. To explore bonding in $Fe(CO)_4SiO$ quantitatively, we must also consider the donating interaction of the 4σ(SiO) MO that lies approximately 3 eV lower in energy than 5σ(SiO). For CO the energy separation between 4σ(CO) and 5σ(CO) is approximately 5 eV. The FMO overlaps of 4σ(SiO) and $Fe(CO)_4$ orbitals of appropriate symmetry are much larger than corresponding overlaps calculated for the 4σ MO of the other diatomic molecules in our study. An FMO diagram for $Fe(CO)_4SiO$ (**1d**, **2d**) (not shown here) indeed reveals that this orbital is substantially involved in bonding. The good σ-donating capabilities of the SiO ligand are due to the excellent overlap of both 4σ and 5σ orbitals, which also lie relatively high in energy compared to CO.

The main interactions involved in π back-bonding, outlined in Figure 4, Scheme 2, and Scheme 3, are those of MOs 2π-(AB) and the $Fe(CO)_4$ fragment orbitals 1e/2e (C_{3v}) and b_1/b_2 (C_{2v}). The fragment orbital overlap values for the C_{3v} and C_{2v} fragment (see Table 3) $Fe(CO)_4$ and AB are generally larger for the fragment orbital overlaps $\langle 2e_1\rvert 2\pi\rangle$ (C_{3v}) and $\langle b_2\rvert 2\pi\rangle$ in comparison to $\langle 1e_1\rvert 2\pi\rangle$ and $\langle b_1\rvert 2\pi\rangle$. This outcome is mainly the consequence of hybridization of Fe 4p into these orbitals and a much better overlap of 4p(Fe) and 2p/3p(A) than for 3d (Fe) and 2p/3p(A).

The π back-bonding components of the $Fe(CO)_4$-AB orbital interactions (ΔE(e) in C_{3v} and $\Delta E(b_1 + b_2)$ in C_{2v}) decrease significantly as we go from CO to the SiO ligand, despite the lower energy of the 2π(AB) acceptor orbital and the somewhat larger $Fe(CO)_4-AB$ overlaps $\langle 2e_1|2\pi\rangle$ (C_{3v}) and $\langle b_2|2\pi\rangle$ (C_{2v}) in the case of SiO. This result may be thought of as an indirect effect of the occupied 1π(AB) MO, which has a repulsive interaction with the π donor MO of $Fe(CO)_4$.[33] We do observe the admixture of 1π(AB) in all cases, but it is most pronounced for SiO because of the relatively high energy of the 1π MO in this diatomic.

C. Bonding in $Fe(AB)_5$. There have been several theoretical studies on $Fe(CO)_5$. One of us[27,29b] has described the bonding in pentacoordinate complexes in general (and $Fe(CO)_5$ in particular) using the extended Hückel method. There are also analyses available using ab initio or DFT methods.[34] A detailed analysis of the complexes $Fe(AB)_5$ is given as Supporting Information, including several tables and figures. Here we discuss only the most important features of what the calculation for the homoleptic $Fe(AB)_5$ shows.

The general trends we noted for the C_{3v}- and C_{2v}-complexes $Fe(CO)_4AB$ can also be observed for $Fe(AB)_5$. The bond dissociation enthalpy BDE (averaged for one Fe−AB bond) reflects the weak coordination of N_2 (34.0 kcal/mol; see Table 1) with respect to CO (56.5); SiO (52.6) is approximately as strongly bound as CO, and BF (75.2) is the strongest ligand of this series. The net charges on the central atom Fe indicate small charge transfer for $Fe(N_2)_5$ (+0.01 electrons) and $Fe(CO)_5$ (−0.07) and thus well-balanced σ donor and π acceptor contributions of the ligands. The large charge-transfer calculated for AB = BF (−0.29) and SiO (−0.32) is a consequence of the better σ donor capabilities of these ligands. We thus conclude that π back-donation of charge is actually smaller than σ donation from AB σ orbitals into metal-centered orbitals.

As already pointed out by Bauschlicher, Siegbahn, and Ziegler and co-workers,[34a−c] it is important to note that in $Fe(CO)_5$ the energetic stabilization due to σ donation from $(CO)_5$ is in fact *less important* than stabilization due to back-donation into $(CO)_5$ accepting orbitals, in line with the corresponding amounts of charge transfer. We find that the same holds true for $Fe(N_2)_5$ and—to a somewhat lesser extent—for $Fe(SiO)_5$ and $Fe(BF)_5$.

D. Vibrational Spectra of $Fe(CO)_4AB$ and $Fe(AB)_5$. As a comparison of the calculated A−B stretching frequencies for the free molecule (Table 5 in the Supporting Information) with the values obtained for the iron complexes **1a** − **3d** (Table 1; see the Supporting Information for $Fe(AB)_5$ complexes) shows, we compute decreased AB frequencies for the N_2 and CO complexes but an increase in the stretching frequencies for the SiO and BF compounds upon ligation. Some experimental evidence for these "upfield shifts" was recently provided by Schnöckel et al.,[12] who studied matrix-isolated [Pd−SiO] (1246 cm^{-1}) and SiO (1226 cm^{-1}) and compared it with [Pd−CO] (2050 cm^{-1}) and CO (2138 cm^{-1}).

CO stretching frequencies in complexes are generally considered a measure of CO bond strength.[3] From previous studies[3] it appears that the CO force constant and thus the CO stretching frequencies are determined primarily by the degree of back-bonding into the CO 2π orbital. MO 2π is strongly C−O antibonding and leads to considerable weakening of the bond, but there is also some effect due to donation from 5σ. As mentioned earlier, we find that the occupied 5σ(AB) orbitals are weakly antibonding, in the order CO > BF > SiO > N_2.

Thus the change in A−B bonding must be considered as the net result of two effects: A−B bond weakening due to back-donation from the $Fe(CO)_4$ fragment into 2π(AB) orbitals and A−B bond strengthening arising from depopulation of the 5σ-(AB) orbital. For N_2 and CO, σ and π orbital interactions with $Fe(CO)_4$ are actually well-balanced. Both orbital interaction energies for σ- and π-interaction displayed in Table 3 are of the same magnitude, but the 2π MOs of N_2 and CO have a pronounced antibonding character. Thus, 5σ(AB) depletion and 2π(AB) population lead to a net weakening of the N_2 and CO bond and a decrease of the stretching frequencies.

In the case of BF and SiO, the orbital interaction of a_1 (σ) symmetry is favored over π orbital mixing and the 2π MOs are much less antibonding. For these diatomics, the effect of depopulation of 5σ(AB) seems to be dominant. The B−F and Si−O bonds become stronger for the complexed diatomic, which leads to an "upfield shift" of the stretching frequency of AB.

6. Conclusions: What Makes CO a Special Ligand and the Incentives for Trying To Make BF and SiO Complexes

What can we say after our detailed discussion of the neutral "10 electron" diatomics AB (N_2, CO, BF, SiO) and their metal complexes $Fe(CO)_4AB$ and $Fe(AB)_5$ about the stability of these compounds? Why is CO so special in organometallic chemistry, to pose our initial question again?

Arguably the main reason for the special character of CO (especially important to the experimentalist) is the excellent balance within this diatomic between its internal stability and its excellent binding. CO has an intermediate HOMO−LUMO gap, which makes it stable—we can handle the stable gas easily in a laboratory—yet moderately reactive. The HOMO of CO, 5σ, an orbital relatively high in energy with a large amplitude on the carbon atom, is most suitable for M−CO bonding. But, as shown in the case of $Fe(CO)_5$, back-bonding into 2π(CO) orbitals is in many cases even more important than σ-donation. It is this balance between donating and accepting capabilities that makes CO a special ligand to transition metals. CO is in many cases strongly bound and inert, a good spectator ligand, but not so inert that it will never react. The 2π acceptor orbital is low enough in energy to enable reactions at the CO ligand, depending on the metal and the ligand environment involved.

The orbital characteristics important for N_2 are a low-lying 5σ (HOMO) and a high-lying 2π orbital (LUMO). As a consequence N_2 is a very stable and inert molecule that binds only weakly to metal complex fragments. Both of the iron compounds $Fe(CO)_4(N_2)$ and $Fe(N_2)_5$ investigated here have been synthesized already[10,11]—they are very labile compounds, characterized in matrix−isolation studies.

Our study suggests that organometallic complexes containing BF or SiO ligands might be experimentally accessible. These ligands have high bonding energies to metal complex fragments. In the case of AB coordination to an $Fe(CO)_4$ fragment, we find bond enthalpies comparable to (AB = SiO), or larger than (AB = BF), those of CO. It does not follow that the resulting complexes $Fe(CO)_4AB$ are kinetically inert, but we are certain that these compounds are not out of reach!

(33) The primary effect of this orbital interaction is a contribution to the Pauli repulsion term ΔE_{Pauli}, but orbital interaction terms can also be affected through an effective reduction of the amplitude of the π donor MO of $Fe(CO)_4$ in the region of the $Fe(CO)_4$−AB bond.

(34) (a) Bauschlicher, C. W.; Bagus, P. S. *J. Phys. Chem.* **1984**, *88*, 5889. (b) Luthi, H. P.; Siegbahn, P. E. M.; Almlöf, J. *J. Phys. Chem.* **1985**, *89*, 2156. (c) Ziegler, T.; Tschinke, V.; Ursenbach, C. *J. Am. Chem. Soc.* **1987**, *109*, 4825. (d) Li, J.; Schreckenbach, G.; Ziegler, T. *J. Am. Chem. Soc.* **1995**, *117*, 486.

We find that SiO is a π acceptor worse than CO but a very good σ donor ligand. So a good strategy might be to avoid electron-rich complex fragments in the synthesis of SiO complexes. SiO complexes especially should be kinetically very labile, due to the high-lying 1π and low-lying 2π orbitals centered on the SiO ligand. But the matrix isolation of more SiO complexes should be possible and an interesting goal for the organometallic chemistry community.

The most interesting ligand in this study is probably BF. Several lines of argument lead us to the conclusion that BF complexes should be (relatively) stable and isolable: (a) The analysis of the isolated diatomics reveals that BF has 5σ donor and 2π acceptor MOs that are more localized on boron than the corresponding frontier orbitals of CO are on carbon, and (b) the HOMO−LUMO gap between 5σ and 2π is smallest in BF. Consistent with these arguments, we find that (c) the bonding metal−AB fragment orbital overlaps, (d) the corresponding orbital interactions ΔE_{oi}, and (e) the overall bond dissociation enthalpies are largest in $Fe(CO)_4BF$.

One has to worry about nucleophilic attack on the boron atom, and a good strategy might be to use bulky ligands to shield the complexed BF ligand. But BF may well also serve as a useful spectator ligand or reaction partner similar to CO. Transition metal valence d orbitals are more strongly involved in an M−BF bond compared to an M−CO bond and so get more stabilized or destabilized, respectively, in BF complexes. Thus the bonding of substrates to metal complexes and the reactivity of these substrates will change, and BF might be a good supplement to CO to control electronic properties of metal complexes that are of interest in homogeneous catalysis. However, it is clear that the isolated ligand BF will be more reactive than CO and, thus, not likely to be of such general utility as CO in the nonreactive saturation of metal valences.

CO and N_2 are stable gases and readily accessible in every laboratory; BF and SiO require special ways of generation and handling techniques. They can be synthesized by high-temperature conproportionation reactions of the elements (boron and silicon) and BF_3 or SiO_2, respectively, and trapped at low temperatures.[35] We are confident that these experimental difficulties will be overcome and that BF and (maybe even more so) SiO complexes will be synthesized in the future.

The present study has encouraged us to investigate theoretically coordination compounds of BF and BO^- as well as the experimentally more easily accessible $B(NH_2)$ and $B(N(CH_3)_2)$ ligands with different mono- and dinuclear metal complex fragments. This study is forthcoming and will be published soon.[14]

Acknowledgment. U.R., F.M.B., and N.G. thank the Deutsche Forschungsgemeinschaft (DFG) for postdoctoral fellowships that made their stay at Cornell University possible. Our work at Cornell was supported by Research Grant CHE 94-08455. A.W.E. wants to thank the DFG for a postdoctoral fellowship that enables him to work in Amsterdam. We want to thank the Cornell Theory Center (CTC) and The Netherlands Organization for Scientific Research (NCF/NWO) for providing grants for supercomputer time.

Supporting Information Available: A detailed analysis of the bonding in $M(AB)_5$ complexes, optimized geometries, and a more detailed presentation of the analysis, in tabular form (19 pages). Ordering information is given on any current masthead page.

IC970897+

(35) (a) Schaschel, E.; Gray, D. N.; Timms, P. L. *J. Organomet. Chem.* **1972**, *35*, 69. (b) Timms, P. L. *J. Am. Chem. Soc.* **1968**, *90*, 4585. (c) Kirk, R. W.; Timms, P. L.; Smith, D. L.; Airey, W. *J. Chem. Soc., Dalton Trans.* **1972**, 1392.